

KRZYSZTOF LABUS*, RADOSŁAW TARKOWSKI**, MAGDALENA WDOWIN***

**Assessment of CO₂ sequestration capacity based
on hydrogeochemical model of Water-Rock-Gas interactions
in the potential storage site within the Belchatów area (Poland)**

Introduction

The PGE Elektrownia Bełchatów S.A. (Bełchatów Power Plant) has started in 2009 a project of the preparatory task to develop a demonstration scale CCS installation within the scope of European Economic Plan for Recovery. The preliminary geological survey and geological structure analyses performed in the Bełchatów area enabled identification of three possible storage sites (the structures of: Wojszyce, Lutomiersk and Budziszewice) (Tarkowski et al. 2009). Current research is aimed at the final choice of the most suitable one. Geochemical modeling is of great importance considering the assessment of geological structures suitability for CO₂ sequestration. Numerous software packages allow for the modeling: eg. PHREEQC (see. Wigand et al. 2008, Sorensen 2009; Tarkowski and Manecki [ed.] 2009), TOUGHREACT (Xu et al. 2001, 2004; Audigane et al. 2005; Xiao 2009), CHILLER, SOLVEQ (Reed et al. 1998; Rosenbauer 2005), Geochemist's Workbench (Zerai 2004; Labus 2008a)). Long-term modeling of CO₂ behavior in contact with geologic formations requires exact data on formation temperature and pressure, petrophysical and petrological parameters of reservoir and cap rock, kinetic parameters of minerals, chemical data of pore fluids, and the time of reaction. This paper presents the results of geochemical modeling for the structure of Budziszewice, performed on the basis of 8 rock samples

* D.Sc., Institute for Applied Geology, Silesian University of Technology, Gliwice, Poland,
e-mail: krzysztof.labus@polsl.pl

** D.Sc. Eng. *** Ph.D. Eng. Mineral and Energy Economy Research Institute of the Polish Academy of Sciences, Kraków, Poland.

TABLE 1
List of analysed rock samples from the Zaosie 2 and the Buków 2 wells

TABELA 1

Wykaz badanych próbek skalnych z otworów Zaosie 2 i Buków 2

No.	Well	Sample no	Depth [m]	Rock type	Total porosity [%]	Porosity from porosimeter [%]	Specific surface [m ² /g]
1.	Zaosie 2	6870	836.50	sandstone	24.45	27.17	0.12
2.	Zaosie 2	6871	838.10	sandstone	26.34	27.15	0.05
3.	Zaosie 2	6872	840.90	sandstone	24.49	26.05	0.14
4.	Zaosie 2	6873	912.40	claystone	6.41	6.05	4.24
5.	Zaosie 2	6874	914.60	claystone	6.39	6.09	4.39
6.	Zaosie 2	6877	1 235.20	mudstone	1.88	1.68	1.25
7.	Buków 2	6892	1 435.60	sandstone	21.68	21.47	0.61
8.	Buków 2	6893	1 436.00	mudstone	6.98	6.46	4.24

(4 samples of the aquifer and 4 of the cap rocks). The samples representing Lower and Middle Jurassic come from the Zaosie 2 and Buków 2 wells, from the depth of 838–1436 m (Table 1). Considering repeatability and amleness of modeling results this study presents results of modeling only for samples 6872 and 6874.

1. Materials and methods

The mineralogical-petrographical examination of samples comprised: microscopic observations (JENALAB Karl Zeiss Jena polarizing microscope – planimetric analysis), SEM-EDS (morphology of grains analysis) and XRD analysis (DRON – 3.0 diffractometer). The X-ray powder diffraction analysis was conducted at $\theta/2\theta$ values 3–74° for Cu K α radiation of wavelength 1.54062 Å, voltage – 34 kV, counter speed – 2°/min. Morphological analysis was performed by means of the Hitachi S-4700 field-emission microscope equipped with a Vantage Noran EDS micro-analytical system and a back-scattered electron detector (YAG BSE).

The aquifer rocks are represented by poorly sorted, loose packed quartz sandstones. Quartz grains, commonly of regular form, are covered with small aggregates of clay minerals. Moreover feldspars and sporadically ore minerals and micas are being observed. Feldspar grains are well preserved with apparent cleavage planes, however kaolinization process is observed in case of some grains. Foliate aggregates of clay minerals (mainly kaolinite) occur in the rocks. The cement occurs in form of clayey-siliceous mass.

Quartz is the dominating component of the cap rocks (aureole of clay minerals are surrounding numerous grains). A significant fraction of feldspars and clay minerals (often

TABLE 2
Mineral assemblages of analysed formations [% vol.]

TABELA 2
Skład szkieletu ziarnowego skał analizowanych formacji [% vol.]

Sample no	6870	6871	6872	6873	6874	6877	6892	6893
Quartz	85.5	86.4	88.6	66.0	70.4	60.7	79.9	46.1
Chalcedony	5.7	3.4	3.2	–	–	20.0	8.3	20.0
Kaolinite	0.6	2.2	0.6	11.0	6.5	8.1	–	4.0
Illite	–	2.0	–	11.0	6.5	8.0	3.8	5.0
Smectite	–	–	–	–	6.5	0.5	–	5.0
Annite	–	–	–	–	–	0.3	–	6.3
Muscowite	0.6	0.3	0.8	–	4.1	0.3	1.3	11.3
K-feldspar	7.6	–	–	–	–	1.2	6.2	1.0
Albite	–	2.8	3.4	8.0	–	–	0.2	–
Anortite	–	2.9	3.4	–	–	–	0.2	–
Goethite	–	–	–	–	3.0	0.9	0.1	1.3
Pyrite	–	–	–	4.0	3.0	–	–	–

regularly formed, tabular grains, of typical hexagonal shape) and micas is also observed. The lamination, that consists in occurrence of quartz laminae alternately with the ones formed of clay minerals or micas, is typical for all of the samples with exception of sample no 6877. Composition of mineral assemblages of analysed formations is presented in the Table 2.

The mean diameter and mean areas of grains were calculated on the basis of the transmitted light pictures except for 3 claystone samples the grain size of which was calculated basing on SEM microphotographs. Mean grain diameter – d, was calculated basing on image analysis results (Mathworks MatLAB 2007b) after the formula:

$$d = 2\sqrt{\frac{S}{\pi}}$$

where: S – grain area.

Specific surfaces of minerals (SSM) were calculated assuming the spherical grain model (Table 3). As the accuracy of image analysis might have been insufficient in case of sandstones' porosimetric properties examination (Labus 2001), the porosity and specific surface was measured by means of mercury porosimetry, those analysis results were taken from the archive of Oil and Gas Institute in Krakow.

TABLE 3
Specific surface of analysed minerals [cm²/g]
TABELA 3
Powierzchnia właściwa analizowanych minerałów [cm²/g]

Sample no	6870	6871	6872	6873	6874	6877	6892	6893
Well	Zaosie 2	Buków 2	Buków 2					
Quartz	2.27	1.89	1.89	226.56	141.60	11.33	3.78	75.52
Chalcedony	68.66	68.66	68.66	—	—	68.66	68.66	75.52
Kaolinite	1 156.49	1 156.49	1 156.49	1 156.49	1 156.49	1 156.49	—	1 156.49
Illite	—	1 085.75	—	1 085.75	1 085.75	1 085.75	1 085.75	1 085.75
Smectite	—	—	—	—	1 031.67	1 031.67	—	1 031.67
Annite	—	—	—	—	—	904.30	—	904.30
Muscovite	105.98	105.98	105.98	—	132.48	105.98	105.98	105.98
K-feldspar	2.35	—	—	—	—	11.73	3.91	78.23
Albite	—	1.91	1.91	229.38	—	—	3.82	—
Anorthite	—	1.81	1.81	—	—	—	3.62	—
Goethite	—	—	—	—	87.87	7.03	4.26	46.86
Pyrite	—	—	—	119.73	74.83	—	—	—

TABLE 4
Groundwater chemistry (basing on the data of Polish Geological Institute and *Assessment of formations...*)

TABELA 4
Informacje dotyczące chemizmu wód złożowych uwzględnionych w modelowaniu
(na podstawie danych z PIG oraz opracowania *Rozpoznanie formacji...*)

Well	Zaosie 2	Zaosie 3
Age	J ₁	J ₁
pH	6.0	7.0
TDS [g/l]	4.62	10.10
Cl ⁻ [mg/l]	709.1	3 900
SO ₄ ²⁻ [mg/l]	396.8	179.20
HCO ₃ ⁻ [mg/l]	159.8	799
CO ₃ ²⁻ [mg/l]	372	300
Ca ²⁺ [mg/l]	400.8	1 442.80
Na ⁺ [mg/l]	350	1 750
K ⁺ [mg/l]	80	120

The formation temperature of the depth interval 900–1000 m was accepted at 36.1°C, and the pore water composition assumed as for the Zaosie 2 well. For the interval 1150–1300 m – temperature at 44.1°C, pore water as for the Zaosie 3 well (Table 4). It was also assumed that the gas fugacity- f_{CO_2} – under hydrostatic pressure reaches 91 bar and 126 bar, respectively.

Geochemical modeling was aimed at characterising sequestration capacity and the changes of rock matrix and the reservoir parameters, that could occur due to CO₂ injection. The simulations were performed with use of Geochemist's Workbench 7.0.1. package in two stages. The first one was aimed at simulating the immediate changes in the aquifer and insulating rocks impacted by the beginning of CO₂ injection (100 days), the second – enabling assessment of long-term effects of sequestration (20 000 years).

2. Results of modeling

2.1. Aquifer rock – an example

The described water-rock-gas interactions were performed for the sample no 6872. At the first stage the CO₂ injection, lasting for 100 days, causes the increase of gas fugacity to the

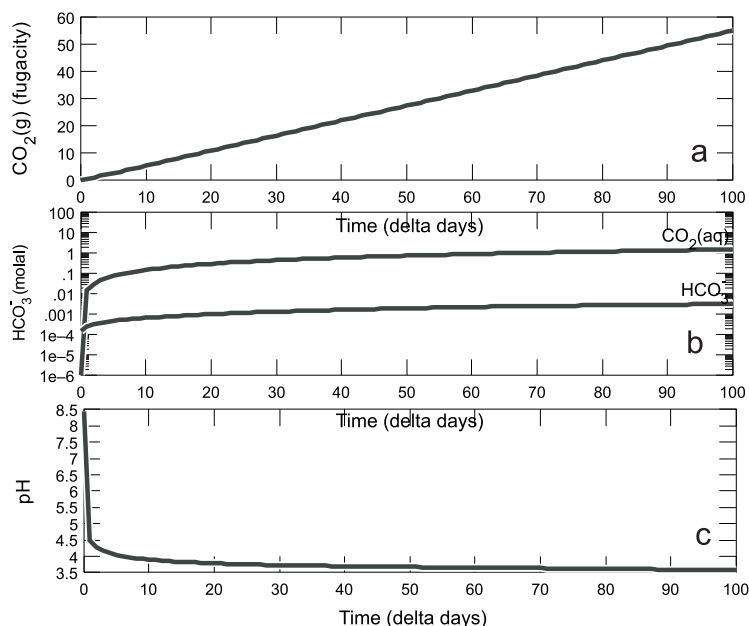


Fig. 1. Changes in: f_{CO_2} , concentrations of CO₂(aq) and HCO₃⁻ and on the stage of CO₂ injection – sample 6872

Rys. 1. Zmiany wartości: a – f_{CO_2} , b – stężeń CO₂(aq) i HCO₃⁻ i c – odczynu pH wód porowych na etapie iniekcji gazu – próbka 6872

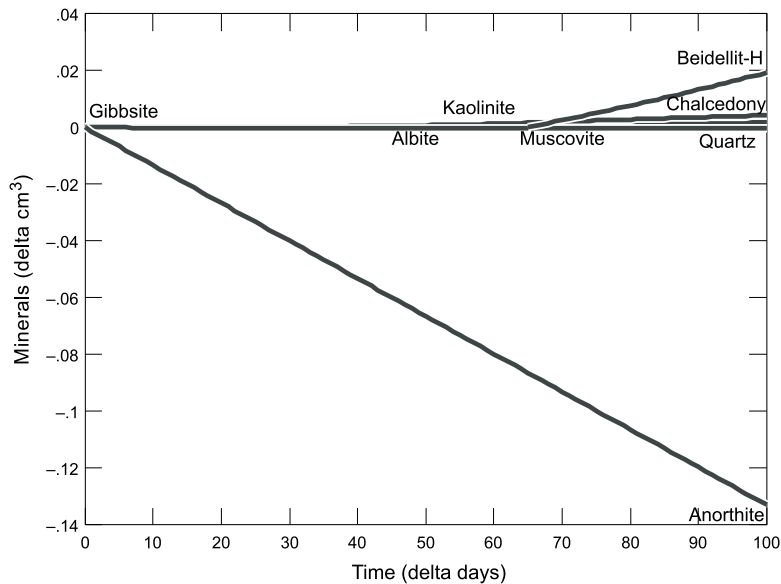


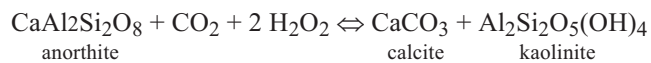
Fig. 2. Changes of minerals quantities on the stage of CO₂ injection – sample 6872

Rys. 2. Zmiany objętości składników mineralnych na etapie wprowadzania gazu – próbka 6872

assumed value: $f_{\text{CO}_2} = 55.2$ bar. In effect a significant elevation of CO_2 (aq) and HCO_3^- concentrations, and a drop of pore waters' reaction to 3.5 pH are observed (Fig. 1). Increase of porosity is controlled by the dissolution of anorthite virtually not influencing the injected fluid penetration into the aquifer. Changes in minerals quantities on the stage of CO_2 injection are shown in the Fig. 2.

In the second stage, CO_2 fugacity drops to the value of about 16 bar (Fig. 3a). The $\text{CO}_2(\text{aq})$ concentrations fall significantly while the ones of HCO_3^- are constant (Fig. 3b); rise of pH reaches the value of 5.4 (Fig. 3c). The porosity decrease, by almost 0.18% (Fig. 3d), might be of slight significance for the permeability of the aquifer.

For the second stage the specific process is the precipitation of calcite and dawsonite (in minor volume) – Fig. 4, 5. Anorthite dissolution is balanced by volume of precipitating of kaolinite. Quantities of mineral phases taking part in these phenomena reactions suggest the following reaction:



Calcite and dawsonite are capable of trapping significant quantities of CO₂ injected (Table 5).

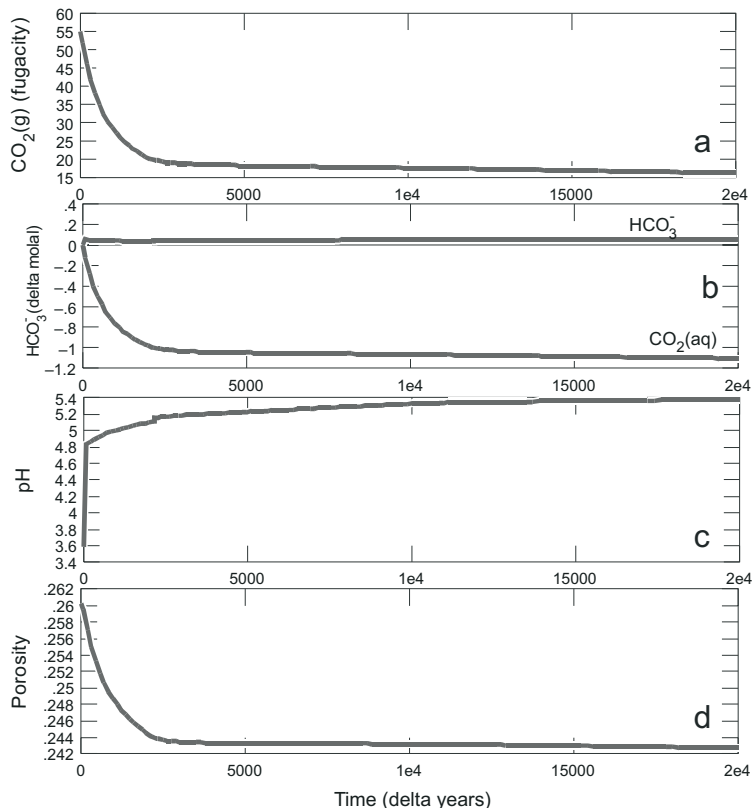


Fig. 3. Changes in: f_{CO_2} , concentrations of $\text{CO}_2(\text{aq})$ and HCO_3^- , pH, and rock matrix porosity since termination of CO_2 injection – sample 6872

Rys. 3. Zmiany po zakończeniu iniekcji gazu:
a – f_{CO_2} , b – stężen $\text{CO}_2(\text{aq})$ i HCO_3^- , c – odczynu pH wód, d – porowatości matrycy skalnej – próbka 6872

2.2. Cap rock – an example

The water-rock-gas interactions were performed for the claystone sample no 6874. Main mechanisms playing the role during the first stage – the CO_2 injection – are different to the ones of the aquifer sandstone sample no 6872. The decrease of pore waters' reaction reaches the value of 3.5 pH (Fig. 6), but the main process is siderite precipitation, that is connected with dissolution of goethite and pyrite. A small decrease of porosity is also observed, due to the volume of newly formed siderite, dominating over the mineral phases being degraded (Fig. 7).

The second stage is characterised by a sudden drop of fugacity (Fig. 8a), $\text{CO}_2(\text{aq})$ (Fig. 8b), and a rapid growth of pH (Fig. 8c). During the first 2000 years of modeling period the concentrations of bicarbonates show strong fluctuations (Fig. 8b). Porosity decreases by nearly 2% (over 30% of the primary value), in favour of the cap rock insulating properties.

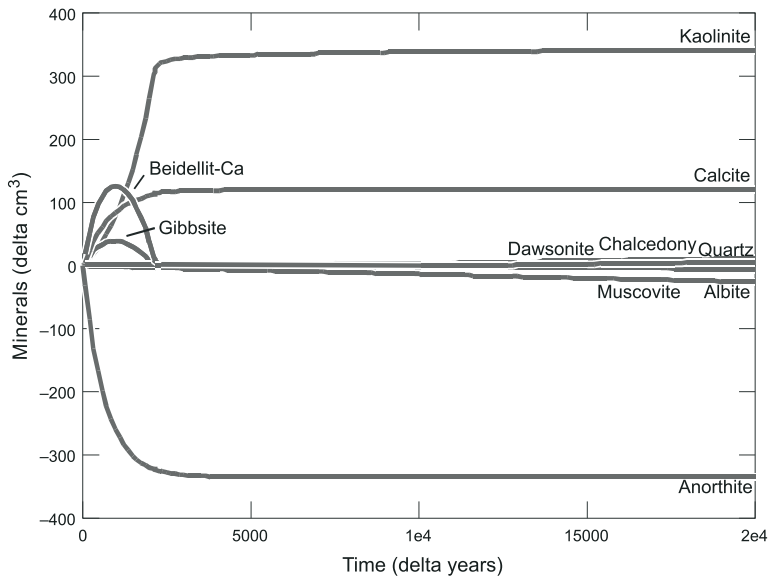


Fig. 4. Changes of minerals volumes after the injection termination – sample 6872

Rys. 4. Zmiany objętości składników mineralnych matrycy skalnej po zakończeniu iniekcji gazu – próbka 6872

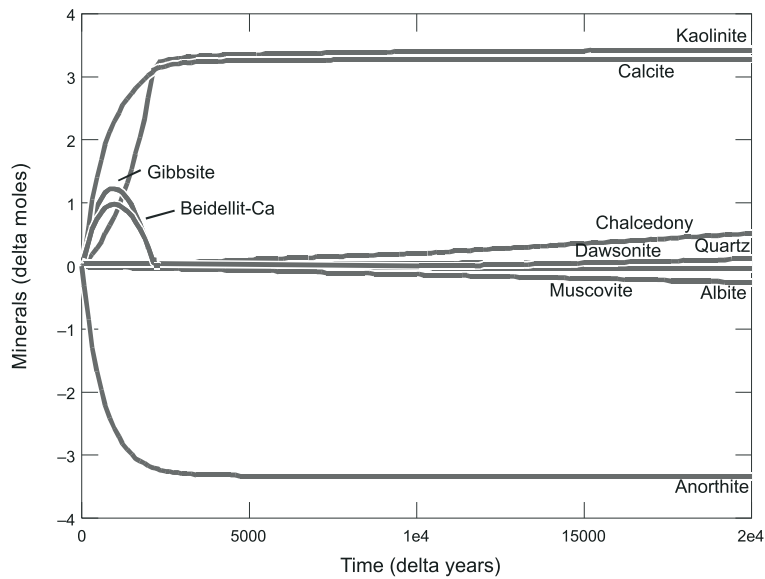


Fig. 5. Changes of minerals quantities after the injection termination – sample 6872

Rys. 5. Zmiany ilości składników mineralnych matrycy skalnej po zakończeniu iniekcji gazu – próbka 6872

Mineral and dissolution trapping capacity of analysed formations

Sekwesuracyjna pojemność mineralna i w roztworze analizowanych formacji

TABLE 5

TABELA 5

	Zaosie 2		Buków 2		Zaosie 2		Zaosie 2		Buków 2			
	6870	6871	6872	6892	Arithmetical mean	Standard deviation	6873	6874	6877	6893	Arithmetical mean	Standard deviation
sandstone	sandstone	sandstone	sandstone	sandstone			claystone	claystone	mudstone	mudstone		
n _p – primary – 0 ka	27.17	27.15	26.05	21.47	25.46	2.71	6.05	6.09	1.68	6.46	5.07	2.27
n _f – final – 20 ka	28.60	28.40	25.70	22.49	26.30	2.86	3.80	5.30	1.64	6.70	4.36	2.17
Dawsonite	–	0.250	0.106	0.104	0.115	0.084	–	–	–	–	–	–
Dolomite	–	–	–	0.014	0.004	–	–	0.12	0.01	–	0.03	0.08
Siderite	–	–	–	–	–	–	–	3.630	0.020	1.227	1.219	1.838
Calcite	–	–	3.065	0.070	0.784	2.118	0.711	–	–	–	–	–
CO ₂ mol/UVR	–	0.250	3.171	0.188	0.902	1.705	0.711	3.750	0.210	1.227	1.475	1.573
Mineral trapping*	kg/m ³	–	0.801	10.32	0.651	2.943	5.540	2.938	15.499	0.924	5.051	6.103
CO ₂ Solubility trapping*	mol/l	0.050	0.068	0.071	0.086	0.069	0.015	5.30E-06	0.020	0.007	4.58E-04	0.007
CO ₂ Solubility trapping*	kg CO ₂ /m ³	0.632	0.845	0.799	0.855	0.783	0.103	8.86E-06	0.048	0.005	0.001	0.014
SUM [kg CO ₂ /m ³]	0.632	1.646	11.119	1.506	3.726	4.949	2.938	15.547	0.929	5.052	6.117	6.508

* – explanations in the text

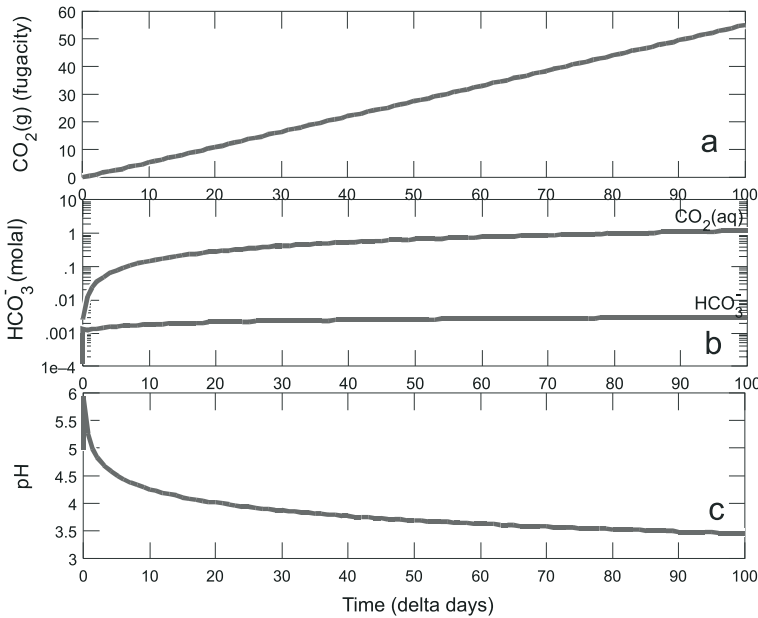


Fig. 6. Changes in: f_{CO_2} , concentrations of $\text{CO}_2(\text{aq})$ and HCO_3^- and on the stage of CO_2 injection – sample 6874

Rys. 6. Zmiany wartości: a – f_{CO_2} , b – stężeń $\text{CO}_2(\text{aq})$ i HCO_3^- i c – odczynu pH wód porowych na etapie iniekcji gazu – próbka 6874

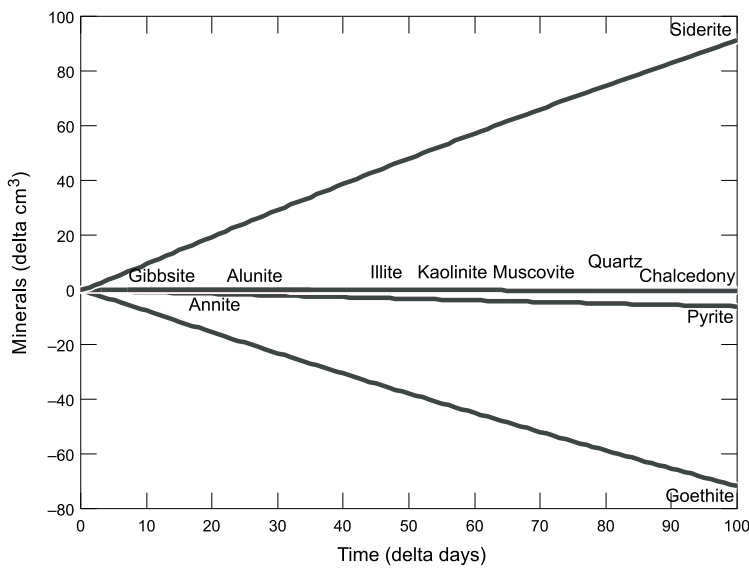


Fig. 7. Changes of minerals quantities on the stage of CO_2 injection – sample 6874

Rys. 7. Zmiany objętości składników mineralnych na etapie wprowadzania gazu – próbka 6874

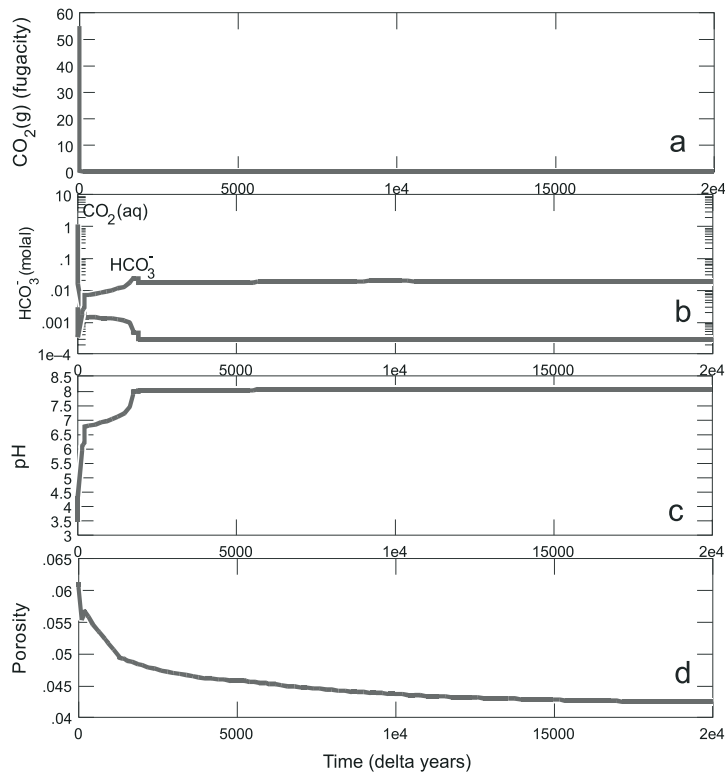


Fig. 8. Changes in: f_{CO_2} , concentrations of $\text{CO}_2(\text{aq})$ and HCO_3^- , pH, and rock matrix porosity since termination of CO_2 injection – sample 6874

Rys. 8. Zmiany po zakończeniu iniekcji gazu
a – f_{CO_2} , b – stężeń $\text{CO}_2(\text{aq})$ i HCO_3^- , c – odczynu pH wód, d – porowatości matrycy skalnej – próbka 6874

Crystallization of nontronite ($(\text{Mg}_{0.16}\text{Fe}_{2}\text{Al}_{0.33}\text{Si}_{3.67}\text{O}_{10})(\text{OH})_2$) – a mineral from the smectite group has a significant meaning for the second stage. This process runs at the cost of another smectite mineral – $(\text{Na}_{0.1}\text{Ca}_{0.25}\text{K}_{0.2}\text{Mg}_{1.1}\text{Fe}_{0.7}\text{Al}_{3.5}\text{Si}_{3.5}\text{O}_{10})(\text{OH})_2$ – assumed to be primarily present in the rock matrix (Fig. 9). Siderite and dolomite are the precipitating mineral phases that are able to efficiently trap injected CO_2 (Fig. 10). It must be underlined that significant amounts of siderite are being formed already at the stage of injection – about $91 \text{ cm}^3 - 3.2 \text{ mol}$; in the stage II – FeCO_3 is supplemented in quantity of 0.85 mol .

3. Sequestration capacity calculations

The trapping capacity of analysed formations (Table 1) was calculated under the following assumptions. The unitary volume of modeled rock -UVR – aquifer or cap rock is equal to 0.01 m^3 and the primary porosity value (prior to storage) is equal to n_p , then the rock

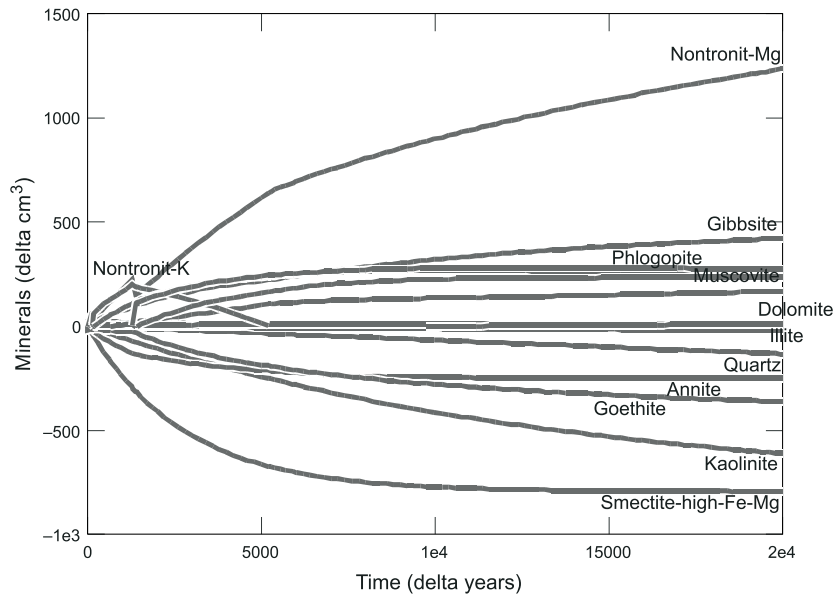


Fig. 9. Changes of minerals volumes after the injection termination – sample 6874

Rys. 9. Zmiany objętości składników mineralnych matrycy skalnej po zakończeniu iniekcji gazu – próbka 6874

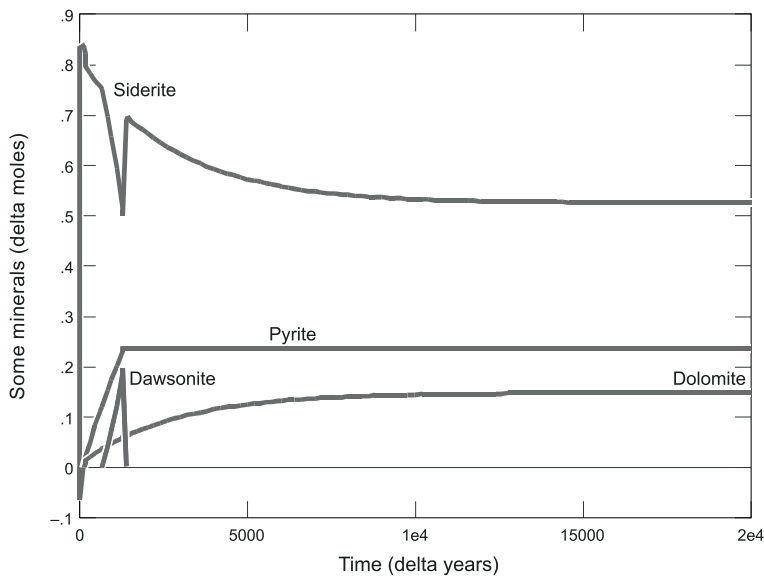


Fig. 10. Precipitation of CO₂ trapping minerals – sample 6874

Rys. 10. Krystalizacja faz zdolnych do mineralnego pułapkowania zatłaczanego dwutlenku węgla – próbka 6874

matrix volume, measured in UVR in 1m^3 of formation is $100(1 - n_p)$. Due to the modeled reactions a certain quantity of carbonate minerals dissolve or precipitate per each UVR. On this basis the CO_2 balance and eventually quantity of CO_2 trapped in mineral phases is calculated. Modeled chemical constitution of pore water allows calculation of the quantity of carbon dioxide trapped in the form of solution. After simulated 20 ka of storage the final porosity is n_f . Pore space is assumed to be filled with pore water of known (modeled) concentrations of CO_2 -containing aqueous species: eg. HCO_3^- , $\text{CO}_2(\text{aq})$, CO_3^{2-} , NaHCO_3 , etc. (expressed in mol HCO_3^-/l).

An example, for the 6873 sample is the following. The primary porosity – n_p is about 0.06, thus 1m^3 of formation contains 94.0 UVRs. For each UVR 0.711 mol of calcite precipitates, trapping 0.711 mol of CO_2 . After 20 ka of storage the final porosity – n_f is equal to 0.038, therefore 1m^3 of formation is assumed to contain 38 dm^3 of pore water. The fluid contains $5.3 \cdot 10^{-6} \text{ mol HCO}_3^-/\text{dm}^3$, then the calculated solution trapping for the formation is $8.86 \cdot 10^{-6} \text{ kg CO}_2/\text{dm}^3$.

Modeling of such water-rock- CO_2 systems requires an extensive theoretical framework and numerous, detailed geochemical input data. The algorithms implemented in the GWB code are not capable to support all of the extensive and complex solutions of effects of multiphase fluid flow, solute transport, changes in porosity and consequently the fluid flow patterns. The applied model results are sensitive to several variables: pore water salinity and composition, pressure, temperature, brine to rock ratio, porosity, reactive surface area, rate of reaction, and rock composition. The quality of the model results may significantly change due to a slight change in any of these quantities. Values of dissolution rates are obtained under laboratory conditions of controlled pH and their effective, field values may be significantly lower. Reactive surface area is estimated basing on the grain size, what is a big simplification taking into account possible factors: as surface roughness, weathering, coatings or the effect of shape. The increase in temperature accelerates the chemical reaction, which creates a favorable condition for more CO_2 to be trapped as carbonates. Mineral dissolution and precipitation rates are a product of the kinetic rate constant and reactive surface area – values of which are highly uncertain and cover a wide range of values. Scaling kinetic rate constants (or reactive surface areas) for all minerals by the same factor is equivalent to scaling the time coordinate. These changes result in reciprocal changes in the time scale (Xu et al. 2003). However, modeling is the cheapest and fastest method of assessment of long-term CO_2 geochemical performance and sequestration capacities of formations.

Conclusions

In the analyzed rock-gas-water systems, in the modeled period of 20 000 years, the minerals able to trap CO_2 are dawsonite, siderite, calcite or dolomite. Mineral-trapping capacity, calculated for the sandstones varies between 0.0 and $11.1 \text{ kg CO}_2/\text{m}^3$, and it is by

10% higher than the value calculated for the Dębowiec Formation aquifer (Miocene of the Upper Silesian Coal Basin – USCB – Poland) (Labus 2008a).

For the cap rocks, the mineral-trapping capacity ranges between 0.9 and 15.4 kgCO₂/m³ – the highest value (sample 6874) is three times higher than in the case of claystones of the Paralic Series (Carboniferous of the USCB) (Labus 2008b).

On the other hand, when interpreting such comparisons, the lower injection depth (about 800 m) and lower formation temperature of the USCB, should be taken into account.

Changes in rock porosity, observed due to the simulation, are insignificant in case of the sandstones. The relative decrease of cap rocks' porosity reaches 40 and 30% (for the sample 6873 and 6874, respectively) to the advantage of their insulating properties.

The presented results proved the occurrence of high sequestration capacity horizons within the analysed area. More exact assessment of the geological space suitability for CO₂ storage requires however the determination of variability of petrophysic and petrological properties and accurate tectonic-structural analysis of the formation.

The researches were made within the national Project: "Assessment of formations and structures for safe CO₂ geological storage, including monitoring plans" made to order of Ministry of The Environment, financed by National Fund for Environmental Protection and Water Management.

REFERENCES

- Audigane P., Gaus I., Pruess, Xu T., 2005 – Reactive transport modeling using TOUGHREACT for the long term CO₂ storage at Sleipner, North Sea. Fourth annual conference on carbon capture and sequestration DOE/NETL, May 2–5, Conferecne proceedings.
- Labus K., 2008a – Możliwości geologicznego składowania CO₂ w utworach formacji dębowieckiej – miocen SW części GZW. Zesz. Nauk. Pol. Śl. Seria: Górnictwo, nr 286, pp. 25–35.
- Labus K., 2008b – Model oddziaływanego z utworami izolującymi CO₂ zatłaczanego do poziomów wodonośnych karbonu GZW. Zesz. Nauk. Pol. Śl. Seria Górnictwo, nr 285. Gliwice, pp. 137–150.
- Labus M., 2001 – Comparison of computer image analysis with mercury porosimetry in sandstone porosity measurement. Geological Quarterly, 45 (1), pp. 75–79.
- Reed M. H., 1998: Calculation of simultaneous chemical equilibria in aqueous-mineral-gas systems and its application to modeling hydrothermal processes. In: Richards J., Larson P., (Eds.), Techniques in Hydrothermal Ore Deposit Geology, Economic Geology, pp. 109–124.
- Rosenbauer R.J., Koksalan T., Palandri J.L., 2005 – Experimental investigation of CO₂-brine-reck interactions at elevated temperature and pressure: Implications for CO₂ sequestration in deep-saline aquifer. Fuel Processing Technology, 86, pp. 1581–1597.
- Rozpoznanie formacji i struktur do bezpiecznego geologicznego składowania CO₂ wraz z ich programem monitorowania. Raport merytoryczny nr 1: Segment I, Rejon Bełchatów, PIG-PIB, Warszawa, czerwiec 2009.
- Sorensen J.A., Holubnyak Y.I., Hawthorne S.B., Miller D.J., Eylangs K., Steadman E.N., Harju J.A., 2009 – Laboratory and numerical modeling of geochemical reactions in a reservoir used for CO₂ storage. Energy Procedia, 1, pp. 3391–3398.
- Tarkowski R., Sylwester M., Uliasz-Misiak B., 2009 – Wstępna geologiczna analiza struktur do składowania CO₂ w rejonie Bełchatowa. Gospodarka Surowcami Mineralnymi, t. 25, z. 2, pp. 37–45.

- Tarkowski R., Manecki M., (red.), 2009 – Badania oddziaływania CO₂ na mezozoiczne skały zbiornikowe w celu określenia ich przydatności do geologicznej sekwestracji dwutlenku węgla. Kraków, IGSMiE PAN.
- Wigand M., Carey J.W., Schütt H., Spangenberg E., Erzinger J., 2008 – Geochemical effects of CO₂ sequestration in sandstones under simulated in situ conditions of deep saline aquifers. *Applied Geochemistry*, 23, pp. 2735–2745.
- Xiao Y., Xub T., Pruess K., 2009 – The effects of gas-fluid-rock interactions on CO₂ injection and storage: insights from reactive transport modeling. *Energy Procedia*, 1, pp. 1783–1790.
- Xu T., Apps J.A., Pruess K., 2003 – Reactive geochemical transport simulation to study mineral trapping for CO₂ disposal in deep arenaceous formations. *Journal of Geophysical Research*, vol. 108, B2, pp. 2071–2084.
- Xu T., Sonnenthal E., Spycher N.F., Pruess K., Brimhall G., Apps A., 2001 – Modeling multiphase fluid flow and reactive geochemical transport in variably saturated fractured rocks: 2 Applications to supergene copper enrichment and hydrothermals flows. *American Journal of Science*, 301, pp. 34–59.
- Xu T., Sonnenthal E., Spycher N.F., Pruess K., 2004 – TOUGHREACT user's guide: A simulation program for non-isothermal multiphase reactive geochemical transport in variable saturated geologic media. Lawrence Berkeley National Laboratory LBNL-55460.
- Zeraf B., Taylor B., Matisoff G., Hanson B., 2004 – Kinetic Modeling and Geochemical Reactions for Sequestration of CO₂ in Deep Saline Aquifer. Third annual conference on carbon capture and sequestration DOE/NETL, May 2–6, Conference proceedings.

OCENA POJEMNOŚCI SKŁADOWANIA CO₂ NA PODSTAWIE MODELOWANIA HYDROGEOCHEMICZNEGO RELACJI WODA-SKAŁA-GAZ W OBREBIE POTENCJALNEGO REPOZYTORIUM W REJONIE BEŁCHATOWA

Słowa kluczowe

Sekwestracja CO₂, modelowanie hydrogeochemiczne, rejon Bełchatowa

Streszczenie

Celem prac była ocena pojemności składowania CO₂ w wybranych poziomach wodonośnych rejonu Bełchatowa oraz określenie efektów oddziaływania tego gazu na zmiany składu oraz porowatości matrycy skalnej. Na wybranych skałach z serii zbiornikowej i skał nadkładu przeprowadzono badania mineralogiczno-petrograficzne: mikroskopowe obserwacje w świetle przechodzącym (analiza planimetryczna), analizę mineralogiczną metodą SEM-EDS (analiza morfologii ziarn), analizę XRD. W modelowaniu geochemicznym, prowadzonym przy zastosowaniu symulatora geochemicznego The Geochemist's Workbench 7.0.1 (GWB), wykorzystano ponadto dane dotyczące porowatości skał oraz parametrów fizykochemicznych solanki występującej na odpowiednich głębokościach. Symulacje przeprowadzono w dwóch etapach. Pierwszy miał na celu modelowanie zmian w skałach zbiornikowych i nadkładu zaraz po rozpoczęciu załączania CO₂ (100 dni), drugi etap – umożliwił oszacowanie długoterminowego wpływu sekwestracji dwutlenku węgla (20 000 lat). Wyniki modelowania w rozpatrywanych układach gaz-woda-skała, w objętym modelowaniem przedziale czasu równym 20 000 lat pokazały, że fazami mineralnymi umożliwiającymi przechwytywanie CO₂ są dawsonit, syderyt, kalcyt i/lub dolomit. Mineralna pojemność sekwestracyjna obliczona na podstawie rezultatów modelowania wynosi dla piaskowców od 0,0 do 11,1 kg/m³ formacji. Dla analizowanych skał uszczelniających mineralna pojemność sekwestracyjna wynosi od 0,9 do 15,4 kg/m³ formacji. Zmiany porowatości skał obserwowane dzięki badaniom modelowym są niewielkie w przypadku piaskowców. Znacznie wyraźniej zaznacza się wzajemny spadek porowatości w skałach drobno-klastycznych – sięgający 40 i 30% (odpowiednio dla próbek 6873 i 6874). Zjawisko to może mieć korzystne znaczenie w punkcie widzenia własności uszczelniających wymienionych skał.

ASSESSMENT OF CO₂ SEQUESTRATION CAPACITY BASED ON HYDROGEOCHEMICAL MODEL OF WATER-ROCK-GAS INTERACTIONS IN THE POTENTIAL STORAGE SITE WITHIN THE BEŁCHATÓW AREA (POLAND)

Key words

CO₂ sequestration, hydrogeochemical modeling, the Bełchatów area

Abstract

Geochemical modeling was aimed at characterising sequestration capacity and the changes of rock matrix and the reservoir parameters, that could occur due to CO₂ injection into possible storage site of the Bełchatów area (Poland). A thorough research of mineralogical and petrophysical parameters of selected reservoir and cap rocks was performed by means of optical microscopy (planimetric analysis), SEM-EDS, XRD. In the simulations which were performed with use of Geochemist's Workbench 7.0.1. package the data of porosity and physico-chemical parameters of brines occurring at the suitable depth were also used. The simulations were performed in two stages. The first one was aimed at simulating the immediate changes in the reservoir and cap rocks impacted by the beginning of CO₂ injection (100 days), the second – enabling assessment of long-term effects of sequestration (20 000 years). Results of modeling in the analysed rock-gas-water systems in considered long-term effects of sequestration (20 000 years) have shown that in the modeled period of 20 000 years, the minerals able to trap CO₂ are dawsonite, siderite, calcite or dolomite. Calculated mineral-trapping capacity for the sandstones varies between 0.0 and 11.1 kgCO₂/m³. For the analysed cap rocks, the mineral-trapping capacity ranges between 0.9 and 15.4 kgCO₂/m³. Changes in sandstones porosity, observed due to the simulation, are insignificant. The significant decrease of fine clastic rocks porosity reaches 40 and 30% (for the sample 6873 and 6874, respectively) to the advantage of insulating properties of the cap rocks.